PHYSICAL REVIEW E **74**, 015202(R) (2006)

Self-organization of chaos synchronization and pattern formation in coupled chaotic oscillators

Xiaoming Zhang,[1] Maolin Fu,[2] Jinghua Xiao,[3] and Gang Hu[4,1,5,*]
[1]*Department of Physics, Beijing Normal University, Beijing 100875, China*
[2]*School of Mathematics and Physics, Nanhua University, Hengyang 421001, China*
[3]*School of Science, Beijing University of Posts and Telecommunications, Beijing 100876, China*
[4]*Chinese Center for Advanced Science and Technology (World Laboratory), Beijing 8730, China*
[5]*Beijing–Hong Kong–Singapore Joint Center of Nonlinear and Complex Systems, Beijing Normal University Branch, Beijing, China*
(Received 11 May 2006; published 18 July 2006)

Pattern formation in spatiotemporal chaotic systems is investigated. Temporally chaotic and spatially ordered patterns are observed by varying the coupling strength. Spatial orderings emerge spontaneously due to self-organization of partial and nonlocal chaos synchronization, governed by various types of spatial symmetries. The first and secondary bifurcations from spatially disordered chaos to chaos with different levels of spatial orderings are observed and the scaling behaviors associated with these bifurcations are statistically analyzed.

DOI: 10.1103/PhysRevE.74.015202 PACS number(s): 05.45.Xt, 82.40.Ck, 82.20.Wt

Chaos has been investigated extensively for more than a half century. In recent decades, the study of spatiotemporal chaos has attracted much attention [1,2]; in particular, the problem of pattern formation in chaotic extended systems has become one of the focuses in nonlinear science [3–7]. Due to the sensitivity of chaotic trajectories to their initial conditions and the unpredictability (i.e., randomness) of the long-time evolutions of chaotic orbits, one can hardly anticipate that chaotic units can construct patterns with strictly ordered space structures. This is the reason why spatial orderings of pattern formation in spatiotemporal chaos have been investigated much less than those of pattern formation in stationary and periodic media [8–13], and thus it is theoretically interesting to investigate the possible formation of patterns in spatiotemporal chaos with ordered space structures.

In this paper, we find that spatially ordered structures can occur spontaneously from spatially disordered and temporally chaotic extended systems by homogeneously increasing space couplings. These spontaneous orderings are due to the self-organization of chaos synchronization and collective behaviors among chaotic units. The self-organization of chaos synchronization is governed by different kinds of space symmetries. Some interesting bifurcations, such as continuous spatial symmetry breaking bifurcation and on-off intermittent bifurcation are found. These bifurcations have been known in stationary and periodic media or in low-dimensional chaotic systems, while in our work we find these critical scaling features among a large number of desynchronous chaotic units, and these features serve as the precursors of self-organization of chaos synchronization.

We take two-dimensional coupled Rössler oscillators with fixed boundary conditions as our example:

$$\dot{u}_{ij} = -v_{ij} - w_{ij} + \varepsilon_u \nabla^2 u,$$

$$\dot{v}_{ij} = u_{ij} + a v_{ij} + \varepsilon_v \nabla^2 v,$$

$$\dot{w}_{ij} = b + w_{ij}(u_{ij} - c) + \varepsilon_w \nabla^2 w,$$

$$\nabla^2 x = x_{i+1,j} + x_{i-1,j} + x_{i,j+1} + x_{i,j-1} - 4x_{ij},$$

$$u,v,w(i=0,j) = u,v,w(i=N+1,j) = 0,$$

$$u,v,w(i,j=0) = u,v,w(i,j=N+1) = 0,$$

$$x = u,v,w; \quad i,j = 1,2,\ldots,N. \tag{1}$$

In our case, the single Rössler oscillator [14] is chaotic, and the coupled oscillators show temporal chaos [Fig. 1(a)] and spatial randomness [Fig. 1(b)] for small coupling strength as one can generally expect.

Now our interest is in what kinds of spatial orderings can spontaneously occur on homogeneously varying the control parameters and how (i.e., via what kinds of bifurcations) these spontaneous orderings appear. To do so we gradually increase the coupling strength $\varepsilon = \varepsilon_u = \varepsilon_v = \varepsilon_w$ of Eqs. (1) and study the system response to this parametric variation. We first find that there exists a critical coupling strength $\varepsilon = \varepsilon_{c1}$, above which a spatial ordering of mirror symmetry

$$u,v,w\left(\frac{N}{2}+i,j\right) = u,v,w\left(\frac{N}{2}-i,j\right),$$

$$0 < i < \frac{N}{2}, \quad 0 < j \le N,$$

$$\text{or} \quad u,v,w\left(i,\frac{N}{2}+j\right) = u,v,w\left(i,\frac{N}{2}-j\right),$$

$$0 < i \le N, \quad 0 < j < \frac{N}{2}, \tag{2}$$

is established (here, if N is odd, we take $(N+1)/2$ to be the central line of the i or j axis). An interesting point is that under the symmetry of Eqs. (2) the system dynamics is still chaotic. In Figs. 2(a)–2(c) we show the snapshots of variables u_{ij} for different time moments, and in Fig. 2(d) the

*Electronic address: ganghu@bnu.edu.cn

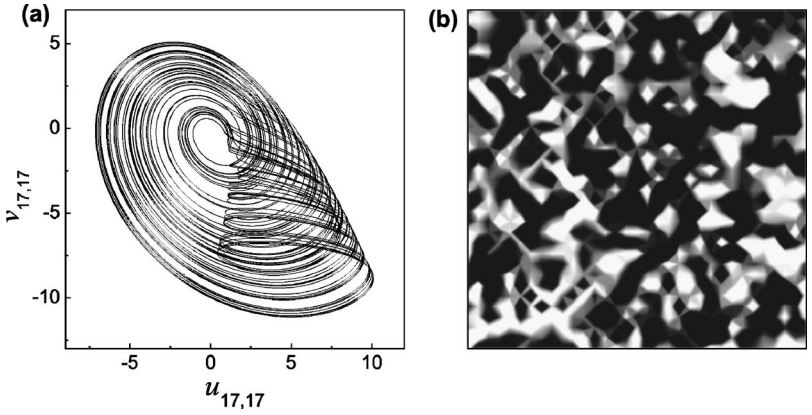

FIG. 1. Chaotic trajectory of a Rössler oscillator and a snapshot of spatiotemporal chaos. Numerical simulations of Eq. (1) start from random initial conditions with the parameter settings $a=0.45$, $b=2.0$, $c=5.5$, $N=33$ (these parameters are fixed in all the following simulations, unless specified otherwise), and $\varepsilon=\varepsilon_u=\varepsilon_v=\varepsilon_w=0.1$. (a) Chaotic temporal evolution of a Rössler oscillator $(i=17,j=17)$. (b) A snapshot of the spatial contour pattern at an arbitrary moment after long transient.

temporal evolution of an arbitrary space site is plotted in the u-v phase plane. It is clear that the trajectory of any space unit is chaotic and the spatial patterns also vary chaotically in time. However, the mirror symmetry (2) is kept in the entire chaotic evolution of Eqs. (1). We thus explore the coexistence of strictly spatial ordering with desynchronous chaotic evolution in a high-dimensional spatiotemporal system. The key point for this interesting observation is partial and nonlocal chaos synchronization [15] self-organized in different clusters governed by the mirror symmetry of Eqs. (2).

On further increasing ε, one can find the second critical coupling strength ε_{c2}, characterizing the secondary bifurcation from the mirror symmetric state (2) to a central symmetric state. In Figs. 2(e)–2(h) we do exactly the same as in Figs. 2(a)–2(d) with ε increased above ε_{c2}. From these figures, we observe again chaotic variations of trajectories as well as chaotic evolution of the spatial pattern. On the other hand, the space central symmetry

$$u,v,w\left(\frac{N}{2}+i,j\right)=u,v,w\left(\frac{N}{2}-i,j\right),$$

$$u,v,w\left(i,\frac{N}{2}+j\right)=u,v,w\left(i,\frac{N}{2}-j\right),$$

and

$$u,v,w\left(\frac{N}{2}+i,\frac{N}{2}+j\right)=u,v,w\left(\frac{N}{2}-i,\frac{N}{2}-j\right)$$

$$0<i<\frac{N}{2},\quad 0<j<\frac{N}{2}, \tag{3}$$

is strictly satisfied during the entire chaotic motion. Now the self-organization of partial chaos synchronization goes to a higher level, and this process is governed by the central symmetry of Eqs. (3), which forms a large symmetry group including the one of Eqs. (2) as partial elements. All symmetry properties of Figs. 2(a)–2(c) and Figs. 2(e)–2(g) are certainly consistent with the system dynamics and the boundary conditions of Eqs. (1). However, whether the system can actually realize these symmetries from initial conditions without such symmetries depends on the competition between temporal chaoticity and spatial couplings. In Fig. 1(b) no spatial symmetry is observed for very weak couplings, while by increasing homogeneous coupling, in Figs. 2(a)–2(c) and 2(e)–2(g), states with mirror and central symmetries become stable successively. In the case of mirror symmetry, the initial distribution determines the actually realized horizontal or vertical symmetry axis.

To explore the general features of the spontaneous orderings in spatiotemporal chaos, we investigate the bifurcation coupling thresholds for different system sizes. In Fig. 3(a)

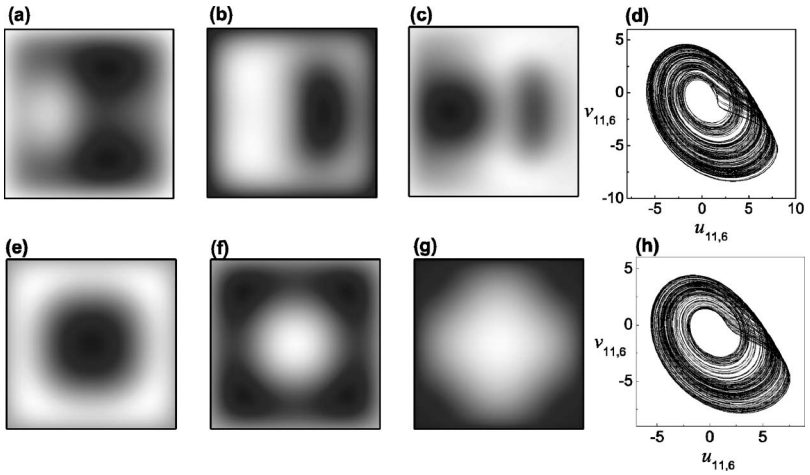

FIG. 2. Chaotic patterns under different coupling strengths and the corresponding chaotic trajectories. (a)–(c) The same as Fig. 1(b) with $\varepsilon=1.91$. The space contour varies chaotically between different patterns with the same mirror symmetry. $t=$(a)30 200, (b) 30 550, and (c) 30 930 t.u.. (d) Chaotic temporal evolution of the trajectory of an arbitrary space site $(i=11,j=6)$. (e)–(g) The same as (a)–(c) with $\varepsilon=2.3$. Chaotic variation of patterns with space ordering of strict central symmetry is observed. $t=$(e)4050, (f) 5700, and (g) 7750 t.u.. (h) The same as (d) with $\varepsilon=2.3$.

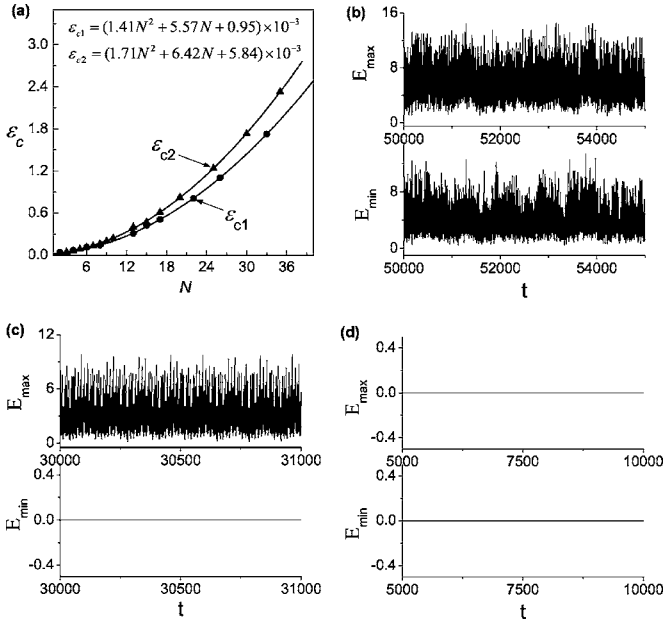

FIG. 3. Quadratic relation between ε_c and N and temporal evolutions of error quantities $E_{\max}, E_{\min}$ defined in Eq. (5). (a) Critical ε_{c1} and ε_{c2} plotted vs system size N. Circles and triangles represent the numerical justifications of ε_{c1} and ε_{c2}, respectively. Solid lines denote analytical quadratic fittings of these critical thresholds. (b) $\varepsilon=1.0<\varepsilon_{c1}$, $E_{\max}>0$, and $E_{\min}>0$. Desynchronous state without spatial symmetry. (c) $\varepsilon_{c1}<\varepsilon=1.91<\varepsilon_{c2}$, $E_{\max}>0$ and $E_{\min}=0$. Chaotic state with mirror symmetry ordering. (d) $\varepsilon=2.3>\varepsilon_{c2}$, $E_{\max}=0$ and $E_{\min}=0$. Chaotic state with central symmetry ordering (i.e., mirror symmetries against both horizontal and vertical axes $i=N/2$ and $j=N/2$).

the two critical couplings ε_{c1} and ε_{c2} are plotted against the system size N. The quadratic power law relations

$$\varepsilon_{c1,c2}=A_{1,2}N^2+B_{1,2}N+C_{1,2} \tag{4}$$

are verified. These relations may be explained heuristically by the second-order diffusion couplings. The continuous version of the coupled oscillators Eqs. (1) is $\dot{\mathbf{u}}=\mathbf{f}(\mathbf{u})+\boldsymbol{\varepsilon}\cdot\nabla^2\mathbf{u}$, which obeys a scaling invariant relation $L\to\alpha L, \varepsilon\to\alpha^2\varepsilon$ with L being the system size of the continuous system. Considering the correspondence $L\propto N$, we can reasonably anticipate the quadratic form Eq. (4), in which the linear and constant corrections may be caused by discretization-induced deviations. When drawing the curves of Fig. 3(a), we justify mirror symmetry and central symmetry by $E_{\min}<10^{-8}$ and $E_{\max}<10^{-8}$ in a time interval over 10^4 time units (t.u.) after a long transient time, with $E_{\min}$ and $E_{\max}$ defined in Eqs. (5). Increasing ε from 0.1 with the step $\Delta\varepsilon=0.01$, ε_1 and ε_2 are plotted and the system is found to transit from no symmetry to mirror symmetry and from mirror symmetry to central symmetry, respectively. From Fig. 3(a), it is obvious that $\varepsilon_{c1,c2}\to\infty$ for $N\to\infty$. Therefore, the phenomena of chaotic spatial orderings of Fig. 2 can be observed in systems with large but finite size rather than in the infinite-size limit, which is sharply different from the pattern formations in conventional stationary or periodic systems. This, however, does not deny the significance of these interesting organization phenomena since the system size effect becomes crucially important in describing the properties of many practically important systems such as confined chemical reaction systems [16], hydrodynamical systems in tiny vessels [17], and various mesoscopic systems [18].

For quantitatively measuring the spatial orderings of Eqs. (2) and (3), we define the following error quantities:

$$E_1(m)=\frac{1}{N}\sum_{i=1}^{N}\left|u\left(i,\frac{N}{2}+m\right)-u\left(i,\frac{N}{2}-m\right)\right|,$$

$$E_2(m)=\frac{1}{N}\sum_{i=1}^{N}\left|u\left(\frac{N}{2}+m,j\right)-u\left(\frac{N}{2}-m,j\right)\right|,$$

$$E_{\min}=\min(E_1(m),E_2(m)),$$

$$E_{\max}=\max(E_1(m),E_2(m)). \tag{5}$$

It is clear that for any $0<m<\frac{N}{2}$ we have

$$E_{\min}>0,\quad E_{\max}>0,\quad \text{no symmetry},$$

$$E_{\min}=0,\quad E_{\max}>0,\quad \text{mirror symmetry Eqs. (2)},$$

$$E_{\min}=0,\quad E_{\max}=0,\quad \text{central symmetry Eqs. (3)}. \tag{6}$$

In Figs. 3(b)–3(d) we choose ε in the ranges of $\varepsilon<\varepsilon_{c1}$, $\varepsilon_{c1}<\varepsilon<\varepsilon_{c2}$, and $\varepsilon>\varepsilon_{c2}$, respectively, and plot $E_{\min}(t)$ and $E_{\max}(t)$ obtained by numerically computing Eqs. (1). The conclusions of Eqs. (6) are fully confirmed by numerical simulations.

In order to clarify the types of bifurcations at ε_{c1} and ε_{c2}, we study the system behaviors in the parameter regions $0<\varepsilon_{ci}-\varepsilon<1$, $i=1,2$. We find that as ε increases toward ε_{c1} from below, $E_{\min}$ decreases continuously [see Figs. 4(a) and 4(b)], and $E_{\min}=0$ as $\varepsilon\geq\varepsilon_{c1}$. Figure 4(c) shows that this continuous decreasing tendency obeys a power law of

$$\bar{E}_{\min}\propto(\varepsilon_{c1}-\varepsilon)^{0.5} \tag{7}$$

where $\bar{E}_{\min}$ is the time average about 4×10^4 t.u. after neglecting a transient of 10^4 t.u. Thus the bifurcation at ε_{c1} is a second-order bifurcation [19] characterized by a symmetry transition. On the other hand, as ε increases toward ε_{c2} from below, a typical on-off intermittency of $E_{\max}$ is observed for $0<\varepsilon_{c2}-\varepsilon\ll1$ [see Figs. 4(d) and 4(e)]. Moreover, the statistics of the off-state period practically follows a $-\frac{3}{2}$ power law at the bifurcation $\varepsilon\approx\varepsilon_{c2}$,

$$P(T)\propto T^{-3/2}, \tag{8}$$

as shown in Fig. 4(f), where T is the time period of an off state between two successive bursts of $E_{\max}$ and $P(T)$ is the probability density of the number of the off states having period T.

When we consider the phase change of the system by increasing ε from $\varepsilon<\varepsilon_{c1}$, we observe successive symmetry bifurcations at ε_{c1} and ε_{c2}. So far, the second-order symmetry breaking bifurcation is well known in spatiotemporal nonchaotic (stationary and periodic) systems and the on-off

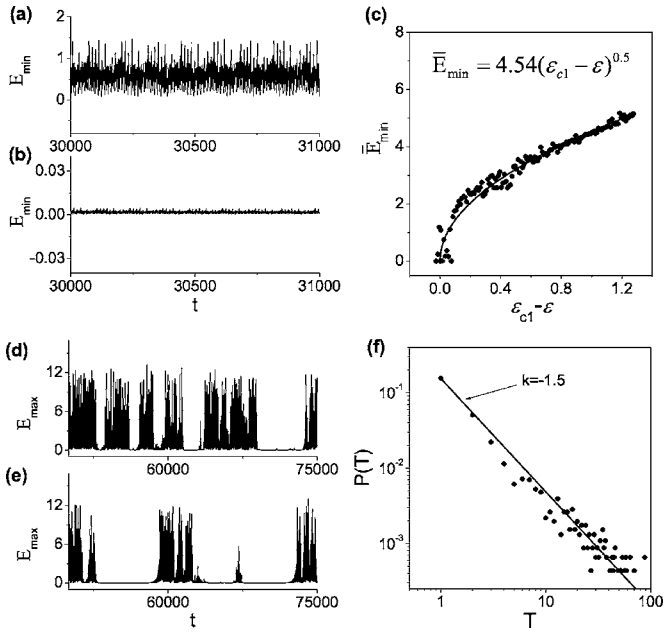

FIG. 4. Temporal evolutions of error quantities E_{max}, E_{min} and power law relations in the neighborhood of two critical points. (a),(b) The same as Fig. 3(b) with E_{min} plotted. (a) $\varepsilon = 1.765$, $\bar{E}_{min} \approx 0.619$. (b) $\varepsilon = 1.78 \lesssim \varepsilon_{c1} \approx 1.785$, $\bar{E}_{min} \approx 0.000883$. (c) $\bar{E}_{min}$ plotted vs $\varepsilon_{c1} - \varepsilon$. A second-order continuous phase transition with scaling relation $\bar{E}_{min} \propto (\varepsilon_{c1} - \varepsilon)^{0.5}$ is justified. (d),(e) The same as Fig. 3(c) with E_{max} plotted. (d) $\varepsilon = 2.06$. (e) $\varepsilon = 2.10 \lesssim \varepsilon_{c2} \approx 2.105$. On-off intermittency of E_{max} variation is justified for $\varepsilon \lesssim \varepsilon_{c2}$. (f) $P(T)$ plotted vs T with T being the time length of an off state between two adjacent E_{max} bursts and $P(T)$ being the probability density of off states having life length T. Typical $T^{-3/2}$ law is obviously observed.

intermittency bifurcation has been justified for desynchronization of homogeneous chaos [20]. Here we explore observation of these bifurcations successively in real space for high-dimensional and spatially disordered spatiotemporal chaotic systems. The fascinating points found here are that the bifurcations of Fig. 4 and the space symmetry orderings of Fig. 2 are realized by self-organization of chaos synchronization between a large number of desynchronous chaotic space units. After the bifurcations chaotic trajectories of space units far away from each other can be organized into some groups in the manner of Eqs. (2) and (3) and the sites in each group are strictly synchronized among each other, leaving large desynchronized space units in between. This organization is spontaneously performed by the system via different instabilities. From Figs. 4(c) and 4(f), it is interesting to see that the bifurcations at ε_{c1} and ε_{c2} belong to two different types. If we use E_{min} and E_{max} as quantitative measures for these two bifurcations, the two quantities have completely different behaviors around the bifurcations. The former shows a continuous reduction of E_{min} with increase of ε (from $\varepsilon < \varepsilon_{c1}$) and E_{min} reduces to zero at ε_{c1}, while the latter maintains the E_{max} amplitude of bursts of on-off intermittency practically unchanged with increase of ε ($\varepsilon < \varepsilon_{c2}$) and the average time interval of off states diverges to infinity as $\varepsilon \to \varepsilon_{c2}$. These features and classifications of bifurcations have been observed in low-dimensional systems. Here we find that these bifurcations and organizations can appear in spatially disordered chaotic extended systems.

In conclusion we have studied the problem of pattern formation in spatiotemporal chaostic systems. The most significant observations are the following. Various strict spatial orderings can be constructed by chaotic units, and these ordered structures are due to the partial chaos synchronization between different clusters of space units self-organized under various spatial symmetries. A second-order symmetry breaking bifurcation and on-off intermittency bifurcation are justified at instabilities of these phase transitions. In this paper the results are reported for a specific Rössler model only. We have tested a number of other models, and similar results are observed, indicating the wide generality of the findings of the present work. We believe that the results in the present work have just touched a small corner of the problem of pattern formation in spatiotemporal chaos. Further investigations on the formation of rich ordered structures and on the diverse transitions between these structures and between different types of spatiotemporal chaos are needed.

This work is supported by National 973 Project of Nonlinear Science and the National Science Foundation of China (Grant No. 10335010).

[1] D. A. Egolf, I. V. Melnikov, W. Pesch, and R. E. Ecke, Nature (London) **404**, 733 (2000).
[2] M. C. Cross and P. C. Hohenberg, Science **263**, 1569 (1994).
[3] L. M. Pecora, Phys. Rev. E **58**, 347 (1998).
[4] G. Hu, Y. Zhang, H. A. Cerdeira, and S. G. Chen, Phys. Rev. Lett. **85**, 3377 (2000).
[5] Z. Liu and Y. C. Lai, Phys. Rev. Lett. **86**, 4737 (2001).
[6] I. Z. Kiss, W. Wang, and J. L. Hudson, Chaos **12**, 252 (2002).
[7] M. Zhan and R. Kapral, Phys. Rev. E **72**, 046221 (2005).
[8] S. H. Strogatz, Physica D **143**, 1 (2000).
[9] Z. G. Zheng, B. B. Hu, and G. Hu, Phys. Rev. E **62**, 402 (2000).
[10] J. N. Blakely, D. J. Gauthier, G. Johnson, T. L. Carroll, and L. M. Pecora, Chaos **10**, 738 (2000).
[11] M. Yoneyama and K. Kawahara, Phys. Rev. E **70**, 021904 (2004).
[12] F. Plenge, H. Varela, and K. Krischer, Phys. Rev. Lett. **94**, 198301 (2005).
[13] I. Z. Kiss, W. Wang, and J. L. Hudson, J. Phys. Chem. B **103**, 11433 (1999).
[14] O. E. Rössler, Phys. Lett. **57A**, 397 (1976).
[15] M. Zhan, Z. G. Zheng, G. Hu, and X. H. Peng, Phys. Rev. E **62**, 3552 (2000).
[16] A. S. Mikhailov and K. Showalter, Phys. Rep. **425**, 79 (2006).
[17] T. M. Squires and S. R. Quake, Rev. Mod. Phys. **77**, 977 (2005).
[18] M. C. Cross and P. C. Hohenberg, Rev. Mod. Phys. **65**, 851 (1993).
[19] P. Chen and M. C. Cross, Phys. Rev. E **56**, 2284 (1997).
[20] S. H. Wang, J. H. Xiao, X. G. Wang, B. B. Hu, and G. Hu, Eur. J. Biochem. **30**, 571 (2002).